ARTICLE

doi:10.1038/nature20166

Bacteria establish an aqueous living space in plants crucial for virulence

Xiu-Fang Xin[1], Kinya Nomura[1], Kyaw Aung[1,2], André C. Velásquez[1], Jian Yao[1]†, Freddy Boutrot[3], Jeff H. Chang[4], Cyril Zipfel[3] & Sheng Yang He[1,2,5,6]

High humidity has a strong influence on the development of numerous diseases affecting the above-ground parts of plants (the phyllosphere) in crop fields and natural ecosystems, but the molecular basis of this humidity effect is not understood. Previous studies have emphasized immune suppression as a key step in bacterial pathogenesis. Here we show that humidity-dependent, pathogen-driven establishment of an aqueous intercellular space (apoplast) is another important step in bacterial infection of the phyllosphere. Bacterial effectors, such as *Pseudomonas syringae* HopM1, induce establishment of the aqueous apoplast and are sufficient to transform non-pathogenic *P. syringae* strains into virulent pathogens in immunodeficient *Arabidopsis thaliana* under high humidity. *Arabidopsis* quadruple mutants simultaneously defective in a host target (AtMIN7) of HopM1 and in pattern-triggered immunity could not only be used to reconstitute the basic features of bacterial infection, but also exhibited humidity-dependent dyshomeostasis of the endophytic commensal bacterial community in the phyllosphere. These results highlight a new conceptual framework for understanding diverse phyllosphere–bacterial interactions.

The terrestrial phyllosphere represents one of the most important habitats on Earth for microbial colonization. Although the vast majority of phyllosphere microbes exhibit benign commensal associations and maintain only modest populations, adapted phyllosphere pathogens can multiply aggressively under favourable environmental conditions and cause devastating diseases. In crop fields, phyllosphere bacterial disease outbreaks typically occur after rainfall and a period of high humidity[1–3], consistent with the 'disease triangle' (host–pathogen–environment) dogma formulated more than 50 years ago[4]. The molecular basis of the effect of high humidity on bacterial infection of the phyllosphere is not understood.

Many plant and animal pathogenic bacteria, including the model phyllosphere bacterial pathogen *Pseudomonas syringae*, carry a type III secretion system (T3SS), which is used to deliver disease-promoting 'effector' proteins into the host cell as a primary mechanism of pathogenesis[5,6]. Studies of how individual type III effectors promote bacterial disease in plants and animals have shown that effector-mediated suppression of host immunity is a common occurrence in both plant–bacterial[7–9] and animal–bacterial interactions[10,11]. However, owing to the apparent molecular complexities in bacterial diseases, which host processes must be impaired for basic bacterial pathogenesis to occur remains unknown in any plant or animal pathosystem.

Immunosuppression and pathogenesis

To investigate whether host immunity may be the only process that needs to be impaired for bacterial pathogenesis to occur in the phyllosphere, we performed infection assays in *Arabidopsis* polymutants that were severely defective in multiple immune pathways: (i) *fls2 efr cerk1* triple mutant (*fec* hereinafter), which is mutated in three major pattern recognition receptor (PRR) genes relevant to *P. syringae* pv. *tomato* strain DC3000 (*Pst*-DC3000) infection[12]; (ii) *bak1-5 bkk1-1 cerk1* triple mutant (*bbc* hereinafter; see Methods), which is compromised in immune signalling downstream of multiple PRRs[13,14]; and (iii) *dde2 ein2 pad4 sid2* quadruple mutant (*deps* hereinafter), which is defective in all three major defence hormone pathways (salicylic acid, jasmonate and ethylene)[15]. Two nonpathogenic mutant derivatives of *Pst*-DC3000 were used: the *hrcC*$^-$ mutant (defective in type III secretion)[16] and the DC3000$^{\Delta 28E}$ mutant, in which the T3SS remains intact, but 28 of 36 type III effectors (Δ28E) are deleted[17]. The *hrcC*$^-$ and DC3000$^{\Delta 28E}$ mutants grew very poorly not only in wild-type *A. thaliana* Columbia-0 (Col-0) (Fig. 1a), but also in immunocompromised mutants when infiltrated into the apoplast, suggesting that host immunity is unlikely to be the only process impaired by *Pst*-DC3000 during infection.

High humidity is required for pathogenesis

During the active pathogenesis phase, phyllosphere bacterial pathogens such as *Pst*-DC3000 live mainly in the air-filled apoplast, which is connected directly to open air through epidermal pores called stomata. The water status inside the apoplast could therefore be influenced by air humidity during pathogen infection. In crop fields, phyllosphere bacterial disease outbreaks typically occur after rainfall and a period of high humidity[1–3,18], consistent with the 'disease triangle' dogma in plant pathology. In addition, one of the earliest and most common symptoms of phyllosphere bacterial diseases is the appearance of 'water soaking' in infected tissues, although whether water soaking has an active role in bacterial pathogenesis remains unclear. Whereas *Pst*-DC3000 multiplied to high numbers under high humidity conditions (approximately 95%; mimicking high humidity after rainfall in crop fields), it multiplied much less under low humidity conditions (<60%) (Fig. 1b), as reflected also by lower disease severity (Fig. 1c). The ability of *Pst*-DC3000 to multiply increased as humidity rose. By contrast, the *hrcC*$^-$ mutant multiplied poorly under all humidity conditions tested (Fig. 1d). The most aggressive infection by *Pst*-DC3000 was associ-

[1]Department of Energy, Plant Research Laboratory, Michigan State University, East Lansing, Michigan 48824, USA. [2]Howard Hughes Medical Institute—Gordon and Betty Moore Foundation, Michigan State University, East Lansing, Michigan 48824, USA. [3]The Sainsbury Laboratory, Norwich Research Park, Norwich NR4 7UH, UK. [4]Department of Botany and Plant Pathology and Center for Genome Research and Biocomputing, Oregon State University, Corvallis, Oregon 97331, USA. [5]Department of Plant Biology, Michigan State University, East Lansing, Michigan 48824, USA. [6]Plant Resilience Institute, Michigan State University, East Lansing, Michigan 48824, USA. †Present address: Department of Biological Sciences, Western Michigan University, Kalamazoo, Michigan 49008, USA.

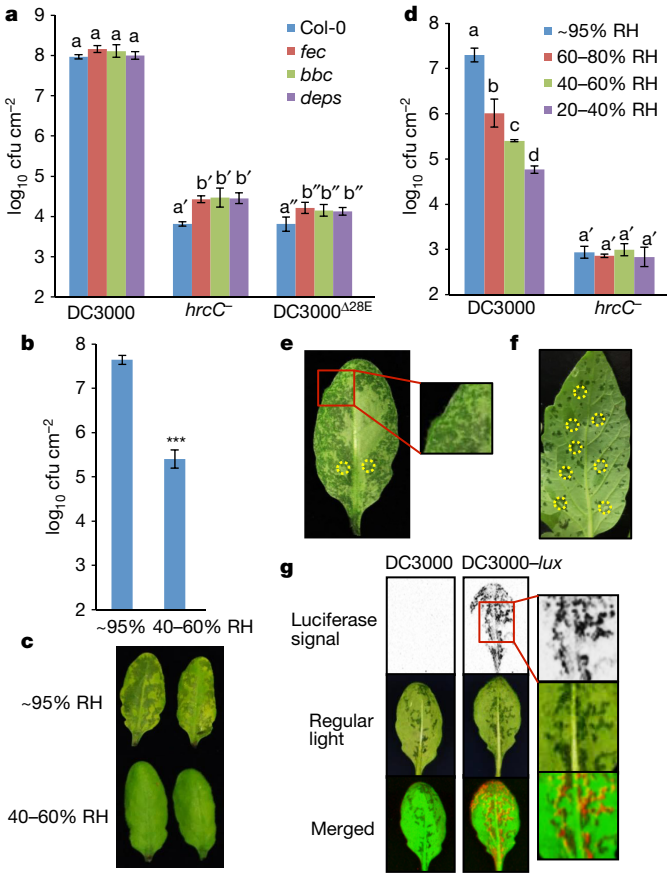

Figure 1 | Full-scale *Pst*-DC3000 infection requires high humidity and is tightly associated with apoplast 'water soaking' **a**, Bacterial populations in Col-0, *fec*, *bbc* and *deps* leaves 2 days after infiltration with bacteria at 1×10^6 cfu ml^{-1}. Humidity: ~95%. Two-way ANOVA with Tukey's test (significance set at $P \leq 0.05$) was performed. No significant differences were found for DC3000 populations in different plant genotypes (indicated by the same letter a), whereas differences were found for the *hrcC*$^-$ or DC3000$^{\Delta 28E}$ populations in different plant genotypes, as indicated by different letters of the same type (a′ versus b′ for *hrcC*$^-$ and a″ versus b″ for DC3000$^{\Delta 28E}$). $n = 4$ technical replicates; data are shown as mean ± s.d. Experiments were repeated three times with similar results. **b**, **c**, Bacterial populations (**b**) and disease symptoms (**c**) 3 days after infiltration with *Pst*-DC3000 at 1×10^5 cfu ml^{-1}. Significant difference was determined by Student's *t*-test (two-tailed); $^{***}P = 1.08 \times 10^{-6}$. $n = 4$ technical replicates; data are shown as mean ± s.d. Experiments were repeated four times with similar results. RH, relative humidity. **d**, Bacterial populations in Col-0 leaves 3 days after infiltration with bacteria at 1×10^5 cfu ml^{-1}. Statistical analysis as in **a**. DC3000 populations showed significant differences under different humidities (as indicated by different letters) whereas *hrcC*$^-$ populations did not (indicated by a′). $n = 3$ technical replicates; data are shown as mean ± s.d. Experiments were repeated three times with similar results. **e**, The abaxial sides of Col-0 leaves 24 h after infiltration with *Pst*-DC3000 at 1×10^6 cfu ml^{-1}. Humidity: ~95%. Dark spots on the leaf indicate water-soaking spots. Red boxes indicate enlarged regions. **f**, A tomato leaf (cv. Castlemart) 3 days after infiltration with *Pst*-DC3000 at 1×10^4 cfu ml^{-1}. Humidity: ~95%. Yellow circles in **e** and **f** indicate infiltration sites. Images are representative of water-soaked leaves from more than four plants. **g**, Col-0 plants were dip-inoculated with bacteria at 2×10^8 cfu ml^{-1}. Humidity: ~95%. Bacterial colonies in inoculated leaves were visualized 2 days later by a charge-coupled device (top) and images of leaves were taken to show water soaking spots (middle). Bottom, merged images, with artificial red colour labelling *Pst*-DC3000–*lux* bacteria. Experiments were repeated three times. Images are representative of leaves from more than four plants.

ated with the appearance, usually within one day after infection, of water soaking in the infected *Arabidopsis* leaves under high humidity (Fig. 1e). Water-soaked spots could also be observed in *Pst*-DC3000-infected leaves of another host species, *Solanum lycopersicum* cv. Castlemart (Fig. 1f). Real-time imaging (Supplementary Video 1) showed that the initial water-soaked spots marked the areas of later disease symptoms (necrosis and chlorosis). It also showed that water soaking was a transient process, which disappeared before the onset of late disease symptoms. Using a *Pst*-DC3000 strain tagged with a luciferase reporter (DC3000–*lux*[19]), we found that water-soaking areas and luciferase signals were detected non-uniformly across the leaf, but they overlapped extensively (Fig. 1g and Extended Data Fig. 1), showing that water-soaked areas are where bacteria multiply aggressively in the phyllosphere before the onset of late disease symptoms.

P. syringae water-soaking effectors

The DC3000$^{\Delta 28E}$ mutant did not cause water soaking under any experimental conditions (for example, high humidity or inoculum). We therefore transformed each of the 28 *Pst*-DC3000 effector genes back into the DC3000$^{\Delta 28E}$ mutant individually, to identify the effector(s) that confer the ability to cause water soaking. Most effectors did not (see Fig. 2a for *avrPto*, as an example), except for *hopM1* and *avrE1*, together with their respective type III secretion chaperones *shcM* and *avrF* (Fig. 2a). This was noteworthy, because although HopM1 and AvrE1 show no sequence similarity, they were previously shown to be functionally redundant in virulence and they are highly conserved in diverse *P. syringae* strains and/or other phytopathogenic bacteria[20,21]. Moreover, transgenic overexpression of 6×His:HopM1 (ref. 22) or 6×His:AvrE1 (ref. 23) in *Arabidopsis*, under the control of a dexamesathone-inducible promoter (10 μM), also caused water soaking under high humidity (Fig. 2b). By contrast, transgenic expression of AvrPto (ref. 29), like the DC3000$^{\Delta 28E}$(*avrPto*) strain, did not induce water soaking. These results show that HopM1 and AvrE1, expressed either by bacteria or by transgenic overexpression in plant cells, are each sufficient to cause water soaking.

Bacterial mutant analysis showed that the *hopM1* and *avrE1* genes are necessary for *Pst*-DC3000 to cause water soaking during infection, whereas the *avrE1*$^-$/*hopM1*$^-$ double mutant[20] could not cause water soaking, even when the inoculum of the *avrE1*$^-$/*hopM1*$^-$ mutant was adjusted to reach a similar population as *Pst*-DC3000 when water soaking was assessed (Fig. 2c). By contrast, *Pst*-DC3000 and the *avrE1*$^-$ and *hopM1*$^-$ single mutants[20] caused strong initial water soaking (Extended Data Fig. 2a) and later disease symptoms (Extended Data Fig. 2b) and multiplied aggressively in a high-humidity-dependent manner, whereas the *avrE1*$^-$/*hopM1*$^-$ double mutant multiplied poorly regardless of humidity conditions (Fig. 2d). Transgenic expression of 6×His:HopM1 in *Arabidopsis* (0.1 nM was used to induce low-level expression of HopM1 so that HopM1 alone does not cause extensive water soaking) greatly enhanced the ability of the *avrE1*$^-$/*hopM1*$^-$ double mutant to cause water soaking and multiply extensively under high humidity conditions (Extended Data Fig. 2c, d). These results showed that, unlike the other 34 effectors present in the *avrE1*$^-$/*hopM1*$^-$ double mutant, the full virulence functions of HopM1 and AvrE1 are uniquely dependent on external high humidity.

Next, we investigated why the virulence functions of HopM1 and AvrE1 were dependent on external humidity. We hypothesized that the primary function of HopM1 and AvrE1 is for creating an aqueous apoplast (that is, bacteria 'prefer' to live in an aqueous environment in the apoplast), the maintenance of which requires high humidity as the leaf apoplast is directly connected to open air through stomata. If so, it may be possible to substitute the function of HopM1 and AvrE1 by simply providing water to the apoplast. To test this hypothesis directly, we performed transient water supplementation experiments in which Col-0 plants infiltrated with the *avrE1*$^-$/*hopM1*$^-$ mutant were transiently kept water-soaked, for the first 12–16 h to mimic the kinetics of transient water soaking that normally occur during *Pst*-DC3000

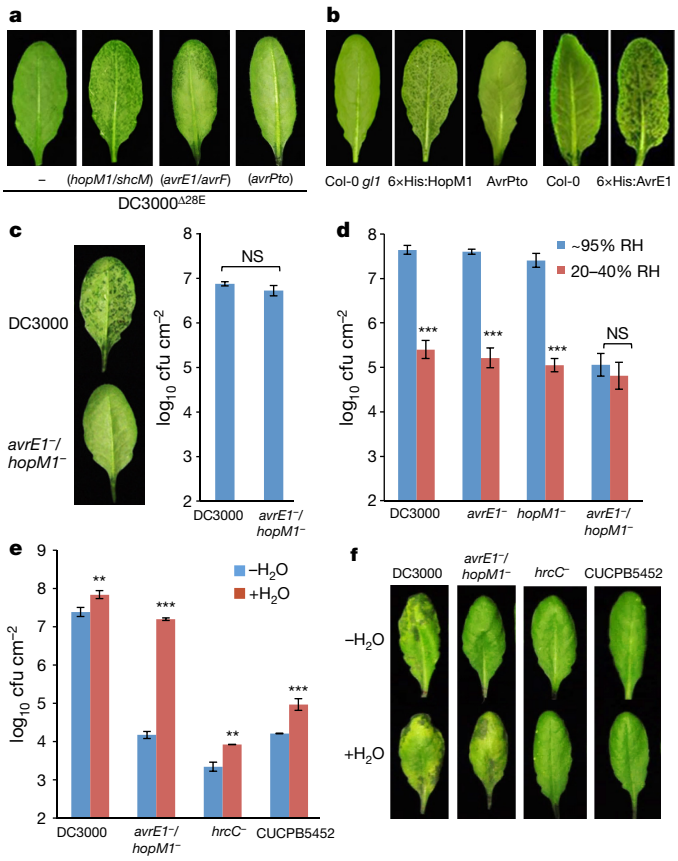

Figure 2 | Type III effectors AvrE1 and HopM1 are necessary and sufficient to cause water soaking. a, Col-0 leaves 24 h after infiltration with bacteria ($1–2 \times 10^8$ cfu ml^{-1}). Humidity: ~95%. **b**, Leaves of transgenic 6×His:HopM1 (ref. 22), 6×His:AvrE1 (ref. 23) or AvrPto (ref. 29) plants after spraying with 10 μM dexamethasone (DEX; to induce effector gene expression). Humidity: ~95%. Col-0 or Col-0 *gl1* (*glabra1*) plants were non-transgenic parental controls. Images are representative of leaves from more than four plants. **c**, Col-0 leaves (left) and bacterial populations (right) 24 h after infiltration with *Pst*-DC3000 (1×10^6 cfu ml^{-1}) or the *avrE1*$^-$/*hopM1*$^-$ strain (1×10^7 cfu ml^{-1}). Humidity: ~95%. Student's *t*-test (two-tailed); NS, not significant ($P = 0.104$). $n = 6$ technical replicates from three independent experiments ($n = 2$ in each experiment); data are shown as mean ± s.d. **d**, Bacterial populations in Col-0 plants 3 days after infiltration with bacteria at 2×10^5 cfu ml^{-1}. ***$P = 1.07 \times 10^{-6}$, 8.07×10^{-7} and 5.95×10^{-7} for DC3000, the *avrE1*$^-$ mutant and the *hopM1*$^-$ mutant, respectively, for differences in bacterial population between different humidities, as determined by Student's *t*-test (two-tailed); NS, not significant ($P = 0.13$). $n = 4$ technical replicates; data are shown as mean ± s.d. Experiments were repeated three times. **e**, **f**, Bacterial populations (**e**) and images (**f**) of Col-0 leaves 3 days after infiltration with bacteria at 1×10^5 cfu ml^{-1}. In the '$-H_2O$' treatment, plants were air-dried normally (for about 2 h) and then kept under high humidity (approximately 95%). In the '$+H_2O$' treatment, plants were kept under high (80–95%) humidity after syringe-infiltration to allow slow evaporation of water (for about 16 h, until no visible apoplast water was seen). **$P = 8.29 \times 10^{-3}$ and 1.14×10^{-3} for DC3000 and *hrcC*$^-$, respectively and ***$P = 7.61 \times 10^{-7}$ and 9.82×10^{-4} for *avrE1*$^-$/*hopM1*$^-$ and CUCPB5452, respectively, indicate significant differences between $-H_2O$ and $+H_2O$ treatments as determined by Student's *t*-test (two-tailed). $n = 3$ technical replicates; data are shown as mean ± s.d. Experiments were repeated three times.

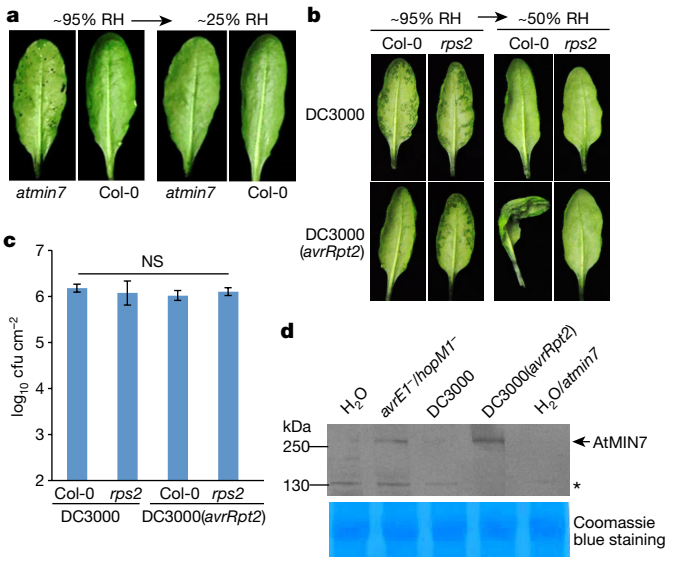

Figure 3 | Effects of AtMIN7 and effector-triggered immunity on water soaking. a, *atmin7* leaves, but not Col-0 leaves, showed partial water soaking 48 h after dip-inoculation with the *avrE1*$^-$/*hopM1*$^-$ mutant at 1×10^8 cfu ml^{-1}. Humidity: ~95%. Water soaking disappeared after transition to low humidity (~25%) to allow evaporation of apoplast water. Images are representative of leaves from more than four plants. **b**, **c**, ETI prevents apoplast water soaking. Col-0 and *rps2* leaves were infiltrated with *Pst*-DC3000 (1×10^6 cfu ml^{-1}) or *Pst*-DC3000(*avrRpt2*) (1×10^7 cfu ml^{-1} for Col-0 and 1×10^6 cfu ml^{-1} for *rps2* plants). Plants were kept under high humidity (~95%) for 24 h to observe water soaking and then shifted to low humidity (~50%) for 4 h to observe ETI-associated tissue collapse. Images were taken before and after low humidity exposure (**b**) and bacterial populations were determined 24 h after infiltration to show similar population levels (**c**). Statistical analysis of data in **c** was performed by one-way ANOVA with Tukey's test (significance set at $P \leq 0.05$), and no significant difference was detected. $n = 3$ technical replicates; data are shown as mean ± s.d. Experiments were repeated three times. **d**, AtMIN7 protein is stabilized during ETI as revealed by immunoblot. Col-0 or *atmin7* leaves were infiltrated with bacteria (1×10^7 cfu ml^{-1}; ref. 25) or H_2O and kept under high humidity (~95%) for 24 h before protein extraction. Asterisk indicates a non-specific band. Coomassie blue staining shows equal loading. See Supplementary Fig. 1 for uncropped images.

infection (Supplementary Video 1). Transient apoplast water supplementation was sufficient to restore the multiplication (100- to 1,000-fold) of the *avrE1*$^-$/*hopM1*$^-$ mutant almost to the level of *Pst*-DC3000 (Fig. 2e), as well as to induce appearance of severe disease symptoms (Fig. 2f). By contrast, the controls, *Pst*-DC3000, the *hrcC*$^-$ mutant and CUCPB5452 (which expresses the *avrE1* and *hopM1* genes but has much reduced virulence owing to deletion of other type III effectors[24]) grew only slightly better (<10 fold) with transient water supplementation (Fig. 2e). These results demonstrate that the primary virulence function of HopM1 and AvrE1 can be effectively substituted by transiently supplying water to the apoplast.

The host target of HopM1 for modulating water soaking

To investigate the mechanism by which HopM1 creates the aqueous apoplast, we focused on the host targets of HopM1 in *Arabidopsis*. We have previously shown that HopM1 is targeted to the trans-Golgi-network–early endosome (TGN/EE) in the host cell and mediates proteasome-dependent degradation of several host proteins, including AtMIN7, which is a TGN/EE-localized ADP ribosylation factor–guanine nucleotide exchange factor involved in vesicle trafficking[22,25,26]. Although the *atmin7* mutant plant showed partially increased bacterial multiplication[22,25], the exact role of AtMIN7 during pathogen infection remains unknown. A previous study showed that the virulence function of HopM1 is fundamentally different from that of canonical immunosuppressing effectors, such as AvrPto[17]. As our data showed a role for HopM1 in creating water soaking, we tested the possibility that AtMIN7 may modulate apoplast water soaking in response to bacterial infection. Notably, we found that apoplast water soaking occurred in the *atmin7* mutant plant in the absence of HopM1/AvrE1 (that is, during infection by the *avrE1*$^-$/*hopM1*$^-$ mutant; Fig. 3a and Extended

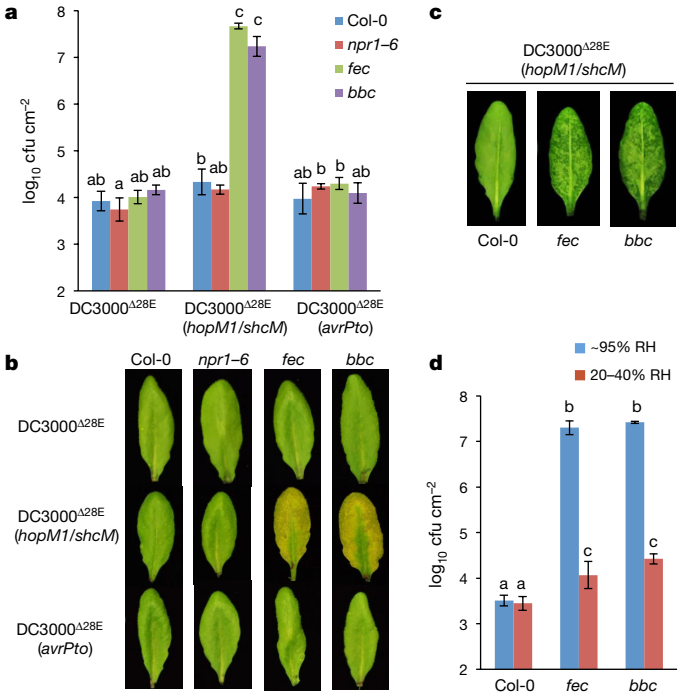

Figure 4 | *hopM1/shcM* transform the non-pathogenic DC3000$^{\Delta 28E}$ mutant into a highly virulent pathogen in PTI-deficient mutant plants in a humidity-dependent manner. a, **b**, Bacterial populations (**a**) and disease symptoms (**b**) 3 days after infiltration with the indicated bacteria at 1×10^6 cfu ml^{-1}. Humidity: ~95%. Statistical analysis was performed by one-way ANOVA with Tukey's test (significance set at $P \leq 0.05$). Bacterial populations indicated by different letters (a, b and c) are significantly different (ab is not significantly different from a or b). $n = 4$ technical replicates; data are shown as mean ± s.d. Experiments were repeated three times. **c**, Water-soaking symptoms were recorded 24 h after inoculation. **d**, Bacterial populations 3 days after infiltration with DC3000$^{\Delta 28E}$(*hopM1/shcM*) at 1×10^6 cfu ml^{-1} under indicated humidities. Statistical analysis as in **a**. Bacterial populations indicated by different letters (a, b and c) are significantly different. $n = 4$ technical replicates; data are shown as mean ± s.d. Experiments were repeated three times. Images are representative of leaves from at least four plants.

Data Fig. 3c), and the *avrE1*$^-$/*hopM1*$^-$ mutant could multiply in *atmin7* mutant plant (Extended Data Fig. 3a, b). Thus, genetic removal of AtMIN7 is sufficient to mimic the virulence function of HopM1, albeit partially, in causing apoplast water soaking. The *atmin7* mutant plant is defective in endocytic recycling of plasma membrane proteins and has an abnormal plasma membrane[26], suggesting that HopM1 degrades AtMIN7, probably to compromise host plasma membrane integrity as a mechanism to create an infection-promoting aqueous apoplast (Extended Data Fig. 4).

If apoplast water soaking is an essential step in pathogenesis, we hypothesized that plants may have evolved defence mechanisms to counter it. Indeed, we found that effector-triggered immunity (ETI)[27] induced by *Pst*-DC3000(*avrRpt2*) blocked water soaking, even when the inoculum of *Pst*-DC3000(*avrRpt2*) was increased to reach a population similar to *Pst*-DC3000 when water soaking was assessed (Fig. 3b, c and Extended Data Fig. 5a, b). When transferred from high (approximately 95%) to low (around 50%) humidity, *Pst*-DC3000(*avrRpt2*)-infected leaves quickly wilted, indicating extensive ETI-associated programmed cell death. By contrast, *Pst*-DC3000-infected, water-soaked leaves returned to pre-infection healthy appearance (Fig. 3b), indicating little host cell death during apoplast water soaking. Furthermore, *Pst*-DC3000(*avrRpt2*)-triggered ETI stabilized the AtMIN7 protein[25] (Fig. 3d). These results therefore show a previously unknown interaction between bacterial virulence (creating apoplast water soaking) and host defence (preventing apoplast water soaking), which is linked in part to AtMIN7 stability, leading to modulation of apoplast water availability.

Reconstitution of *P. syringae* infection

As apoplast water soaking seems to be a key process in bacterial pathogenesis, we investigated a model in which suppression of pattern-triggered immunity (PTI) and creation of apoplast water soaking are two principal pathogenic processes sufficient for bacterial infection of the phyllosphere to occur. We infected Col-0 and two PTI-compromised triple mutant plants (*fec* and *bbc*) with DC3000$^{\Delta 28E}$, DC3000$^{\Delta 28E}$(*avrPto*) or DC3000$^{\Delta 28E}$(*hopM1/shcM*) and found that DC3000$^{\Delta 28E}$(*hopM1/shcM*), but not DC3000$^{\Delta 28E}$ or DC3000$^{\Delta 28E}$(*avrPto*), caused strong water soaking, multiplied aggressively (almost to the level of *Pst*-DC3000) and produced prominent disease symptoms in the *fec* and *bbc* mutant plants (Fig. 4a–c) in a high humidity-dependent manner (Fig. 4d). Furthermore, unlike PTI mutants, the *npr1-6* mutant plant, which is defective in salicylic-acid-dependent defence (Extended Data Fig. 6a–c), did not show greatly increased DC3000$^{\Delta 28E}$(*hopM1/shcM*) multiplication (Fig. 4a). Thus, a combination of defective PTI and the presence of an aqueous-apoplast-inducing effector (HopM1) could almost fully convert a non-pathogenic mutant into a virulent pathogen in the *Arabidopsis* phyllosphere.

If immunosuppression and creation of apoplast water soaking are two principal pathogenic processes sufficient for bacterial infection of the phyllosphere, we hypothesized that it might be possible to construct a multi-host-target mutant that simulates the two processes. This mutant plant might allow an otherwise non-pathogenic mutant bacterium (for example, the *hrcC*$^-$ mutant) to colonize the phyllosphere, thereby reconstituting basic features of a phyllosphere bacterial infection. For this purpose, we mutated the *AtMIN7* gene in PTI mutants (*fec* and *bbc*) and generated *atmin7 fls2 efr cerk1* (*mfec* hereinafter) and *atmin7 bak1-5 bkk1-1 cerk1* (*mbbc* hereinafter) quadruple mutants using CRISPR–Cas9 technology (see Methods and Extended Data Fig. 7a). The quadruple mutant plants display a similar morphology to wild-type Col-0 plants (Extended Data Fig. 7b) and have a tendency to show some water-soaking spots, especially in mature leaves, under high humidity (Extended Data Fig. 7c, d). Notably, these mutants allowed the non-pathogenic *hrcC*$^-$ mutant to multiply aggressively under high (approximately 95%) humidity, to a final population that was about 100-fold higher than in Col-0 plants 5 days after inoculation, with the *mbbc* plants showing a greater susceptibility than the *mfec* plants (Fig. 5a). In addition, in these quadruple mutant plants, the *hrcC*$^-$ mutant induced prominent disease chlorosis and necrosis (Fig. 5b and Extended Data Fig. 7e), which were not observed for the *hrcC*$^-$ strain in Col-0, *atmin7* or PTI mutants. Thus, dual disruption of AtMIN7 and PTI signalling is sufficient to generate the basic features of a model phyllosphere bacterial disease. Consistent with these data, transient water supplementation to the leaf apoplast was sufficient to enhance the growth of the *hrcC*$^-$ mutant in the *bbc* triple mutant, but not in Col-0 plants (Fig. 5c). To our knowledge, this is the first infectious model disease, in plant or animal, for which basic pathogenesis has been generated using biologically relevant host-target mutants.

Dyshomeostasis of commensal bacteria

The inability of the non-pathogenic *hrcC*$^-$ mutant to multiply aggressively in the wild-type phyllosphere resembles that of the commensal bacterial community that resides in the apoplast of healthy leaves. Consistent with this, only low levels of the endophytic phyllosphere bacterial community were detectable in wild-type Col-0 plants (Fig. 5d). However, after plants were shifted from regular growth conditions (around 60% relative humidity, day 0; Fig. 5d) to high humidity conditions (approximately 95% relative humidity), the *mfec* and *mbbc* quadruple mutant plants, but not Col-0 plants, showed excessive proliferation of the endogenous endophytic bacterial community

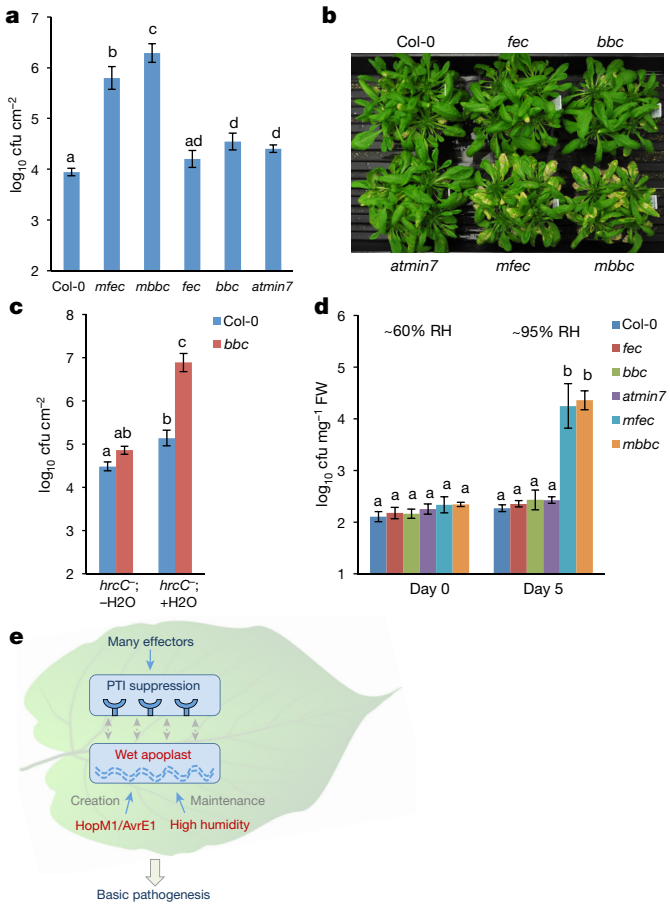

Figure 5 | Disease reconstitution experiments. a, **b**, *hrcC*$^{-}$ bacterial populations 5 days (**a**) and disease symptoms 10 days (**b**) after dip-inoculation in Col-0, *fec*, *bbc*, *atmin7*, *mfec* and *mbbc* plants grown in Redi-Earth soil. Humidity: ~95%. Statistical analysis was performed by one-way ANOVA with Tukey's test (significance set at $P \leq 0.05$). Bacterial populations indicated by different letters (a, b, c and d) are significantly different (ad is not significantly different from a or d). $n = 4$ technical replicates; data are shown as mean ± s.d. Experiments were repeated four times. **c**, *hrcC*$^{-}$ bacterial populations in Col-0 and *bbc* leaves 3 days after infiltration with bacteria at 1×10^6 cfu ml^{-1}. The $-H_2O$ and $+H_2O$ conditions are as in Fig. 2e. Statistical analysis was performed by one-way ANOVA with Tukey's test (significance set at $P \leq 0.05$). Bacterial populations indicated by different letters (a, b and c) are significantly different (ab is not significantly different from a or b). $n = 3$ technical replicates; data are shown as mean ± s.d. Experiments were repeated three times. **d**, Col-0, *fec*, *bbc*, *atmin7*, *mfec* and *mbbc* plants grown in *Arabadopsis* Mix soil were mock-sprayed with H_2O and kept under high humidity (~95%). On day 0 (before water spray) and day 5, total populations of the endophytic bacterial community were quantified by counting CFUs on R2A plates, after surface sterilization of leaves with 75% ethanol, leaf homogenization and serial dilutions. FW, fresh weight. Statistical analysis as in **a**. Bacterial populations indicated by different letters (a and b) are significantly different. $n = 4$ technical replicates; data are shown as mean ± s.d. Experiments were repeated three times. **e**, A proposed new model for *Pst*-DC3000 pathogenesis in *Arabidopsis*. Dashed arrows indicate a possible interaction, at spatial and temporal scales, between 'immunosuppression' and a 'wet apoplast' during pathogenesis.

(Fig. 5d and Extended Data Table 1), in a high-humidity-dependent manner (Extended Data Fig. 8a). Furthermore, the excessive proliferation of the endophytic bacterial community was associated with mild tissue chlorosis and necrosis in some leaves (Extended Data Fig. 8b). This was noteworthy, because a recent study showed that overgrowth of a beneficial root-colonizing fungus in immunocompromised (against fungal pathogens) plants also led to harmful effects in *Arabidopsis*[28], illustrating a potentially common occurrence where the levels of commensal and beneficial microbiota must be strictly controlled by the host for optimal plant health. It would be interesting in the future to conduct comprehensive *in planta* 16S rRNA amplicon-based analysis to determine whether there are also humidity-dependent changes in the composition of commensal bacterial communities in the Col-0, *mfec* and *mbbc* plants.

Discussion

Our data suggest a new conceptual framework for understanding phyllosphere–bacterial interactions (Fig. 5e). Specifically, we have identified PTI signalling and AtMIN7, presumably via vesicle trafficking, as two key components of the elusive host barrier that functions to limit excessive and potentially harmful proliferation of non-pathogenic microbes (for example, the *hrcC*$^{-}$ mutant) in the phyllosphere. Pathogenic bacteria, such as *Pst*-DC3000, have evolved T3SS effectors not only to disarm PTI signalling but also to establish an aqueous living space in a humidity-dependent manner in order to aggressively colonize the phyllosphere. The conceptual framework presented here integrates host, pathogen and environmental factors, and provides a critical insight into the basis of the strong effect of humidity on the development of numerous bacterial diseases, consistent with the 'disease triangle' dogma in plant pathology.

Prior to this study, humidity was commonly thought to promote bacterial movements on the plant surface and invasion into plant tissues. Our study, however, reveals a notable and previously unrecognized effect of high humidity on the function of bacterial effectors inside the plant apoplast. An aqueous apoplast could potentially facilitate the flow of nutrients to bacteria, promote the spread and/or egression of bacteria, and/or affect apoplastic-host-defence responses, the latter of which may underlie some of the previously observed effects of HopM1, AvrE1 and AtMIN7 on plant immunity[21,23,25] and suggest a potential cross-talk between plant immune responses and water availability.

Most of our current knowledge on plant–pathogen and plant–microbiome interactions are derived from studies under limited laboratory conditions. This study illustrates a need for future research to consider the dynamic climate conditions in which plants and microbes live in nature in order to uncover new biological phenomena involved in host–microbe interactions. Research that unravels the molecular bases of environmental influences of disease development should help us to understand the severity, emergence and/or disappearance of infectious diseases in crop fields and natural ecosystems, especially in light of the rapidly changing drought–humidity patterns associated with global climate change.

Online Content Methods, along with any additional Extended Data display items and Source Data, are available in the online version of the paper; references unique to these sections appear only in the online paper.

Received 9 May; accepted 17 October 2016.

1. Miller, S., Rowe, R. & Riedel, R. Bacterial spot, speck, and canker of tomatoes. *Ohio State University Extension Fact Sheet HYG-3120–96* (1996).
2. Pernezny, K. & Zhang, S. Bacterial speck of tomato. *University of Florida IFAS Extension PP-10* (2005).
3. Schwartz, H. F. Bacterial diseases of beans. *Colorado State University Extension. Fact Sheet No: 2.913*. (2011).
4. Stevens, R. B. *Plant Pathology, an Advanced Treatise.* Vol. 3, 357–429 (Academic, 1960).
5. Büttner, D. & He, S. Y. Type III protein secretion in plant pathogenic bacteria. *Plant Physiol.* **150,** 1656–1664 (2009).
6. Galán, J. E. & Collmer, A. Type III secretion machines: bacterial devices for protein delivery into host cells. *Science* **284,** 1322–1328 (1999).
7. Asai, S. & Shirasu, K. Plant cells under siege: plant immune system versus pathogen effectors. *Curr. Opin. Plant Biol.* **28,** 1–8 (2015).
8. Dou, D. & Zhou, J. M. Phytopathogen effectors subverting host immunity: different foes, similar battleground. *Cell Host Microbe* **12,** 484–495 (2012).
9. Macho, A. P. & Zipfel, C. Targeting of plant pattern recognition receptor-triggered immunity by bacterial type-III secretion system effectors. *Curr. Opin. Microbiol.* **23,** 14–22 (2015).
10. Asrat, S., Davis, K. M. & Isberg, R. R. Modulation of the host innate immune and inflammatory response by translocated bacterial proteins. *Cell. Microbiol.* **17,** 785–795 (2015).

11. Sperandio, B., Fischer, N. & Sansonetti, P. J. Mucosal physical and chemical innate barriers: lessons from microbial evasion strategies. *Semin. Immunol.* **27,** 111–118 (2015).
12. Gimenez-Ibanez, S., Ntoukakis, V. & Rathjen, J. P. The LysM receptor kinase CERK1 mediates bacterial perception in *Arabidopsis*. *Plant Signal. Behav*. **4,** 539–541 (2009).
13. Macho, A. P. & Zipfel, C. Plant PRRs and the activation of innate immune signaling. *Mol. Cell* **54,** 263–272 (2014).
14. Schwessinger, B. *et al.* Phosphorylation-dependent differential regulation of plant growth, cell death, and innate immunity by the regulatory receptor-like kinase BAK1. *PLoS Genet.* **7,** e1002046 (2011).
15. Tsuda, K., Sato, M., Stoddard, T., Glazebrook, J. & Katagiri, F. Network properties of robust immunity in plants. *PLoS Genet.* **5,** e1000772 (2009).
16. Yuan, J. & He, S. Y. The *Pseudomonas syringae* Hrp regulation and secretion system controls the production and secretion of multiple extracellular proteins. *J. Bacteriol.* **178,** 6399–6402 (1996).
17. Cunnac, S. *et al.* Genetic disassembly and combinatorial reassembly identify a minimal functional repertoire of type III effectors in *Pseudomonas syringae*. *Proc. Natl Acad. Sci. USA* **108,** 2975–2980 (2011).
18. Hirano, S. S. & Upper, C. D. Population biology and epidemiology of *Pseudomonas syringae*. *Annu. Rev. Phytopathol.* **28,** 155–177 (1990).
19. Fan, J., Crooks, C. & Lamb, C. High-throughput quantitative luminescence assay of the growth in planta of *Pseudomonas syringae* chromosomally tagged with *Photorhabdus luminescens* luxCDABE. *Plant J.* **53,** 393–399 (2008).
20. Badel, J. L., Shimizu, R., Oh, H. S. & Collmer, A. A *Pseudomonas syringae* pv. *tomato* avrE1/hopM1 mutant is severely reduced in growth and lesion formation in tomato. *Mol. Plant Microbe Interact.* **19,** 99–111 (2006).
21. DebRoy, S., Thilmony, R., Kwack, Y. B., Nomura, K. & He, S. Y. A family of conserved bacterial effectors inhibits salicylic acid-mediated basal immunity and promotes disease necrosis in plants. *Proc. Natl Acad. Sci. USA* **101,** 9927–9932 (2004).
22. Nomura, K. *et al.* A bacterial virulence protein suppresses host innate immunity to cause plant disease. *Science* **313,** 220–223 (2006).
23. Xin, X. F. *et al. Pseudomonas syringae* effector Avirulence protein E localizes to the host plasma membrane and down-regulates the expression of the *NONRACE-SPECIFIC DISEASE RESISTANCE1/HARPIN-INDUCED1-LIKE13* gene required for antibacterial immunity in *Arabidopsis*. *Plant Physiol.* **169,** 793–802 (2015).
24. Wei, C. F. *et al.* A *Pseudomonas syringae* pv. *tomato* DC3000 mutant lacking the type III effector HopQ1-1 is able to cause disease in the model plant *Nicotiana benthamiana*. *Plant J.* **51,** 32–46 (2007).
25. Nomura, K. *et al.* Effector-triggered immunity blocks pathogen degradation of an immunity-associated vesicle traffic regulator in *Arabidopsis*. *Proc. Natl Acad. Sci. USA* **108,** 10774–10779 (2011).
26. Tanaka, H., Kitakura, S., De Rycke, R., De Groodt, R. & Friml, J. Fluorescence imaging-based screen identifies ARF GEF component of early endosomal trafficking. *Curr. Biol.* **19,** 391–397 (2009).
27. Whalen, M., C., Innes, R. W., Bent, A. F. & Staskawicz, B. J. Identification of *Pseudomonas syringae* pathogens of *Arabidopsis* and a bacterial locus determining avirulence on both *Arabidopsis* and soybean. *Plant Cell* **3,** 49–59 (1991).
28. Hiruma, K. *et al.* Root endophyte *Colletotrichum tofieldiae* confers plant fitness benefits that are phosphate status dependent. *Cell* **165,** 464–474 (2016).
29. Hauck, P., Thilmony, R. & He, S. Y. A *Pseudomonas syringae* type III effector suppresses cell wall-based extracellular defense in susceptible *Arabidopsis* plants. *Proc. Natl Acad. Sci. USA* **100,** 8577–8582 (2003).

Supplementary Information is available in the online version of the paper.

Acknowledgements We thank He laboratory members for insightful discussions and constructive suggestions. We thank J. Kremer for help with setting up real-time disease imaging experiments and advice on 16S rRNA amplicon sequencing, K. Sugimoto for providing tomato plants (cv. Castlemart), and C. Thireault for technical help. This project was supported by funding from Gordon and Betty Moore Foundation (GBMF3037), National Institutes of Health (GM109928) and the Department of Energy (the Chemical Sciences, Geosciences, and Biosciences Division, Office of Basic Energy Sciences, Office of Science; DE–FG02–91ER20021 for infrastructural support). C.Z. acknowledges support from The Gatsby Charitable Foundation.

Author Contributions X.-F.X., K.N. and S.Y.H. designed the experiments. K.A. performed the *Pst*-DC3000–*lux* imaging experiment. A.C.V. performed biological repeats of bacterial infection experiments shown in Fig. 1a. J.Y. characterized an unpublished plant mutant line. X.-F.X. and K.N. performed all other experiments, including bacterial infections, protein blotting and generation of Arabidopsis *mfec* and *mbbc* mutant lines. F.B. and C.Z. contributed unpublished plant mutant materials. J.H.C. contributed unpublished *Pst*-DC3000 effector constructs. X.-F.X. and S.Y.H. wrote the manuscript with input from all co-authors.

Author Information Reprints and permissions information is available at www.nature.com/reprints. The authors declare no competing financial interests. Readers are welcome to comment on the online version of the paper. Correspondence and requests for materials should be addressed to S.Y.H. (hes@msu.edu).

Reviewer Information *Nature* thanks G. Beattie, S. Lindow, J.-M. Zhou and the other anonymous reviewer(s) for their contribution to the peer review of this work.

METHODS

Plant materials and bacterial strains. *Arabidopsis thaliana* plants were grown in *Arabidopsis* Mix soil (equal parts of SUREMIX (Michigan Grower Products Inc.), medium vermiculate and perlite; autoclaved once) or Redi-Earth soil (Sun Gro Horticulture) in environmentally controlled growth chambers, with relative humidity at 60%, temperature at 22 °C and a 12 h light–12 h dark cycle. Five-week-old plants were used for bacterial inoculation and disease assays.

The *bak1-5 bkk1-1 cerk1* mutant plant was generated by crossing the *bak1-5 bkk1-1* mutant[14] with the *cerk1* mutant[30]. PCR-based genotyping was performed in F_2 progeny to obtain a homozygous triple mutant. The *npr1-6* (Fig. 4a) mutant was the SAIL_708_F09 line ordered from the *Arabidopsis* Biological Resource Center, and confirmed to be a knockout mutant and defective in salicylic acid signalling (Extended Data Fig. 6).

Bacterial disease assays. Syringe-infiltration and dip-inoculation were performed in this study. Briefly, *Pst*-DC3000 and mutant strains were cultured in modified Luria–Bertani medium (10 g l^{-1} tryptone, 6 g l^{-1} yeast extract, 1.5 g l^{-1} KH_2PO_4, 0.6 g l^{-1} NaCl, and 0.4 g l^{-1} $MgSO_4{\cdot}7H_2O$) containing 100 mg l^{-1} rifampicin (and/or other antibiotics if necessary) at 28 °C to an OD_{600} of 0.8–1.0. Bacteria were collected by centrifugation and re-suspended in sterile water. Cell density was adjusted to $OD_{600} = 0.2$ (approximately 1×10^8 cfu ml^{-1}). For syringe-infiltration, bacterial suspension was further diluted to cell densities of 1×10^5–1×10^6 cfu ml^{-1}. Unless stated otherwise, infiltrated plants were first kept under ambient humidity for 1–2 h for water to evaporate, and after the plant leaves returned to pre-infiltration appearance, plants were kept under high humidity (approximately 95%; by covering plants with a clear plastic dome) or other specified humidity settings for disease to develop. For dip-inoculation, plants were dipped in the bacterial suspension of $OD_{600} = 0.2$, with 0.025% Silwet L-77 added, and then kept under high humidity (approximately 95%) immediately for disease to develop.

Different humidity settings were achieved by placing a clear plastic dome over a flat (in which plants are grown) with different degrees of opening. A humidity–temperature Data Logger (Lascar) was placed inside the flat to record the humidity and/or temperature over the period of disease assay.

For quantification of *Pst*-DC3000 bacterial populations, *Arabidopsis* leaves were surface-sterilized in 75% ethanol and rinsed in sterile water twice. Leaf disks were taken using a cork borer (9.5 mm in diameter) and ground in sterile water. Colony-forming units were determined by serial dilutions and plating on Luria-Marine plates containing 100 mg l^{-1} rifampicin. One technical replicate consists of one or two leaf disks and 3 or 4 technical replicates (that is, from at least 3 or 4 leaves) were included in each biological experiment. Experiments were repeated at least three times.

CRISPR–Cas9-mediated mutation of the *AtMIN7* gene. The one-plasmid CRISPR–Cas9 cloning system[31] was used to mutate *AtMIN7* into the *fls2 efr cerk1* and *bak1-5 bkk1-1 cerk1* plants. *AtMIN7*-single guide (sg)RNA primers containing target mutation regions were as follows, with *AtMIN7* sequence underlined.

AtMIN7-sgRNA-F, GATTGATCATTTGGAAGGGGATCC; *AtMIN7*-sgRNA-R, AAACGGATCCCCTTCCAAATGATC.

The constructs containing *AtMIN7*-sgRNA and *Cas9* were cloned in pCAMBIA1300, which were then mobilized into *Agrobacterium tumefaciens* for plant transformation. For genotyping of *AtMIN7*-mutated lines, total DNA was extracted from individual lines and the regions containing the CRISPR target sites were amplified by PCR using the following primers:

AtMIN7-sgRNA-F2, GATGCTGCTTTGGATTGTCTTC; *AtMIN7*-sgRNA-R2, AATGGCTCCCCATGCACTGCGATA.

For genotyping, the PCR products were digested with the *Bam*HI restriction enzyme and plant lines showing an (partially or completely) uncut band were chosen. The PCR products of putative homozygous T_2 lines, identified based on a lack of cutting by *Bam*HI, were sequenced. The lines showing a frame-shift mutation and an absence of the *Cas9* gene based on PCR using the following primers were identified as homozygous lines. The T_3 and T_4 progeny of homozygous lines were used for disease assays. Primers for PCR-amplifying *Cas9* gene were as follows:*Cas9*-F, CCAGCAAGAAATTCAAGGTGC; *Cas9*-R, GCACCAGCTGGATGAACAGCTT.

Imaging of bacterial colonization with luciferase assay. Four-week-old *Arabidopsis* Col-0 plants were dip-inoculated with the *Pst*-DC3000 or *Pst*-DC3000–*lux* strain[19]. The infected plants were fully covered with a plastic dome to maintain high humidity. Leaves were excised from the infected plants 2 days after inoculation and the light signals were captured by a charge-coupled device (CCD) using ChemiDoc™ MP system (Bio-Rad).

AtMIN7 protein blot. *Arabidopsis* leaves were syringe-infiltrated with bacteria or H_2O and kept under high humidity (approximately 95%) for 24 h. Leaf disks were homogenized in 2× SDS buffer, boiled for 5 min and centrifuged at 10,000*g* for 1 min. Supernatants containing the total protein extracts were subjected to separation by SDS–polyacrylamide gel electrophoresis (PAGE). An AtMIN7 antibody[22] was used for western blotting to detect the AtMIN7 protein. Uncropped blot and gel images are included in Supplementary Fig. 1.

Bacterial community quantification. Five-week-old plants were sprayed with H_2O and covered with a plastic dome to keep high humidity (approximately 95%) for 5 days. To quantify the endophytic bacterial community, leaves were detached, sterilized in 75% ethanol for 1 min (Extended Data Fig. 9) and rinsed in sterile water twice. Leaves were weighed and ground in sterile water using a TissueLyser (Qiagen; at the frequency of 30 times per second for 1 min) in the presence of 3-mm Zirconium-oxide grinding beads (Glen Mills; 5 beads in each tube). After serial dilutions, bacterial suspensions were plated on R2A plates (Teknova), which were kept at 22 °C for 4 days before colonies were counted. Colony-forming units were normalized to tissue fresh weight.

16S rRNA amplicon sequence analysis of the endophytic bacterial community. The Col-0, *mfec* and *mbbc* plants were sprayed with water and kept under high humidity (approximately 95%) for 5 days. Leaves were surface-sterilized in 75% ethanol for 1 min and rinsed in sterile water twice. Leaves from four plants were randomly selected (2 leaves from each plants; 8 leaves in total) and were divided into 4 tubes (2 leaves in each tube) and ground in sterile water. Bacterial suspensions were diluted (Col-0 samples were diluted to 10^{-3} and *mfec* and *mbbc* samples were diluted to 10^{-5}) and, for each genotype, 15 μl suspension from each tube of the right dilution (10^{-3} dilution for Col-0 and 10^{-5} for *mfec* and *mbbc*) were pooled together and plated on R2A plates, which were kept at 22 °C for 4 days. Fifty colonies from each genotype were randomly picked, genomic DNA was extracted and PCR was performed with AccuPrime high-fidelity Taq DNA polymerase (Invitrogen) and primers 799F/1392R (ref. 32) to amplify bacterial 16S rRNA gene. The PCR product was sequenced and taxonomy of each bacterium (family level) was determined by Ribosomal Database Project at Michigan State University (https://rdp.cme.msu.edu/)[33].

Data analysis, statistics and experimental repeats. The experiments were not randomized and the investigators were not blinded to allocation during experiments and outcome assessment. The specific statistical method used, the sample size and the results of statistical analyses are described in the relevant figure legends. Sample size was determined based on experimental trials and with consideration of previous publications on similar experiments to allow for confident statistical analyses. The Student's two-tailed *t*-test was performed for comparison of means between two data points. A one-way or two-way ANOVA with Tukey's test was used for multiple comparisons within a data set, with significance set to a P value ≤ 0.05. ANOVA analysis was performed with GraphPad Prism software.

Data Availability. The bacterial 16S rRNA sequences in Extended Data Table 1 have been deposited in the National Center for Biotechnology Information (NCBI) GenBank database under accession numbers KX959313–KX959462. Other data that support the findings of this study are available from the corresponding author upon request.

30. Miya, A. *et al.* CERK1, a LysM receptor kinase, is essential for chitin elicitor signaling in *Arabidopsis*. *Proc. Natl Acad. Sci. USA* **104,** 19613–19618 (2007).
31. Feng, Z. *et al.* Multigeneration analysis reveals the inheritance, specificity, and patterns of CRISPR/Cas-induced gene modifications in *Arabidopsis*. *Proc. Natl Acad. Sci. USA* **111,** 4632–4637 (2014).
32. Bai, Y. *et al.* Functional overlap of the *Arabidopsis* leaf and root microbiota. *Nature* **528,** 364–369 (2015).
33. Wang, Q., Garrity, G. M., Tiedje, J. M. & Cole, J. R. Naive Bayesian classifier for rapid assignment of rRNA sequences into the new bacterial taxonomy. *Appl. Environ. Microbiol.* **73,** 5261–5267 (2007).

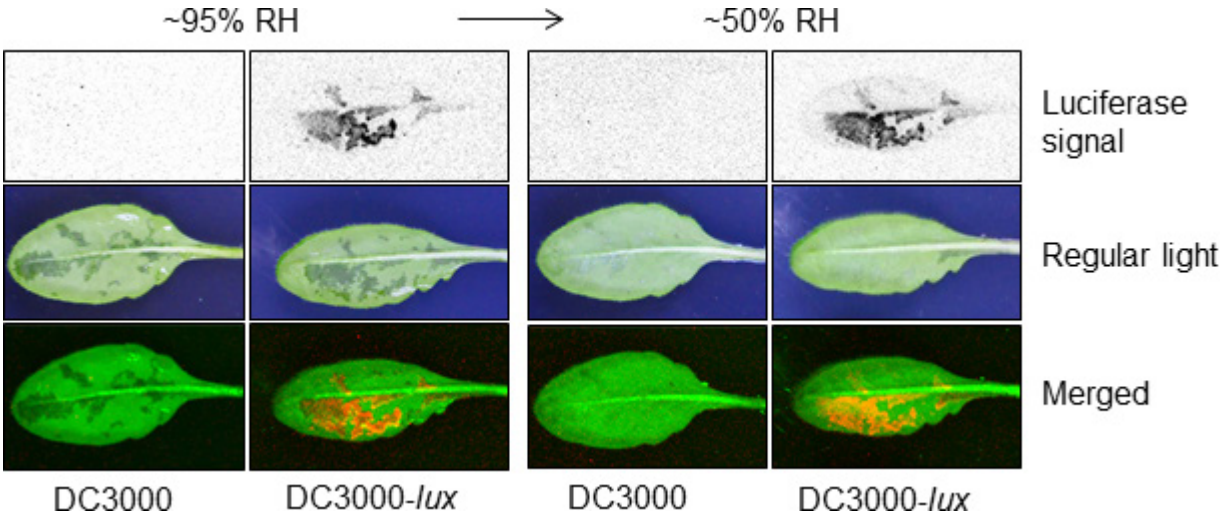

Extended Data Figure 1 | Water soaking does not affect luminescence signal. Col-0 plants were dip-inoculated with bacteria at 2×10^8 cfu ml^{-1} and kept under high humidity (approximately 95%) for 2 days. Imaging was performed in the same way as in Fig. 1g. Water-soaked leaves were air-dried for about 2 h and imaged again (right panel). Images are representative of leaves from more than four plants.

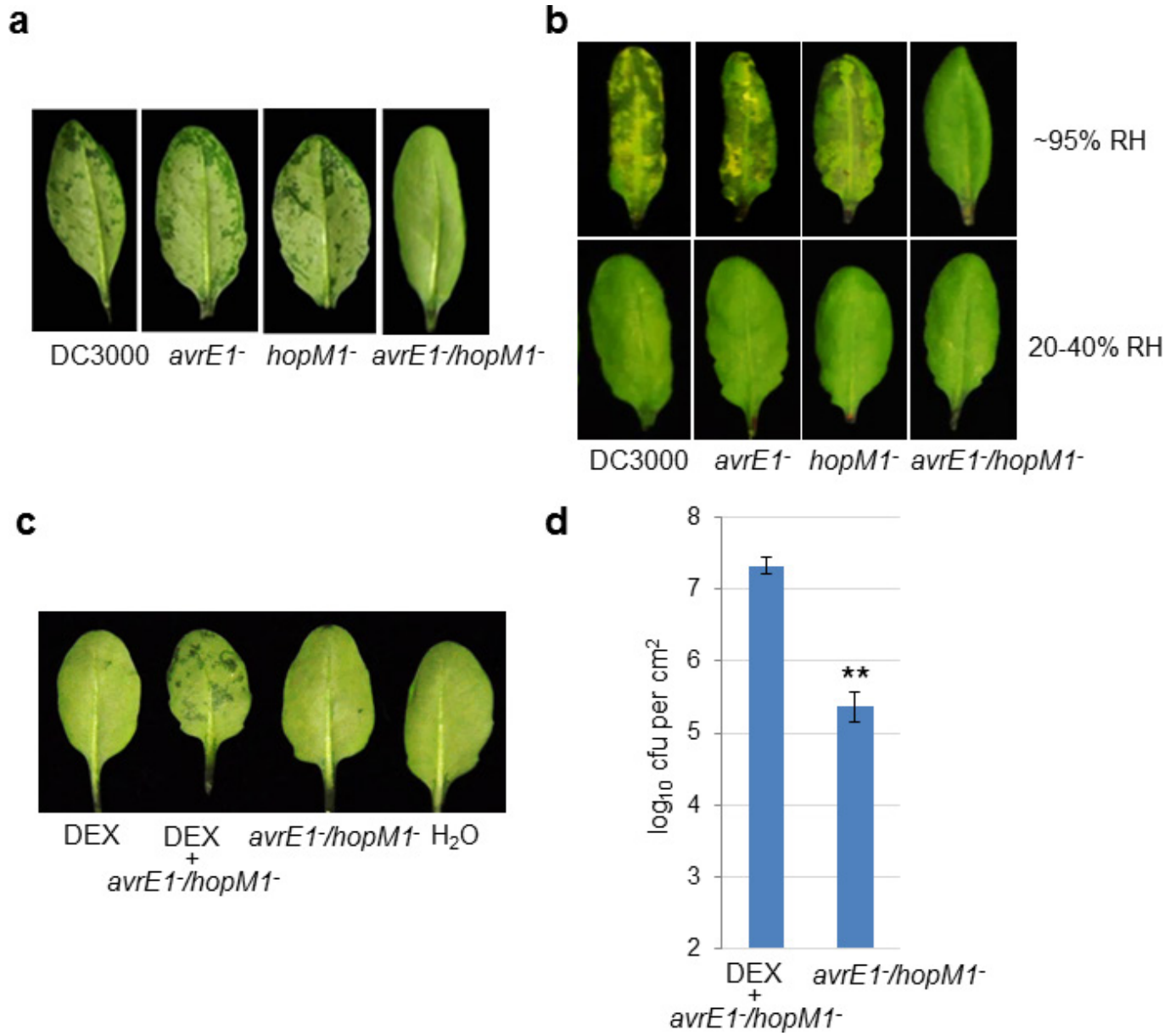

Extended Data Figure 2 | Humidity dependence of HopM1/AvrE1 function and restoration of the virulence of the *avrE1*$^{-}$*/hopM1*$^{-}$ mutant in 6×His:HopM1 transgenic plants. a, b, The virulence of the *avrE1*$^{-}$*/hopM1*$^{-}$ mutant is insensitive to humidity settings. **a**, Col-0 plants were syringe-infiltrated with indicated bacteria at 2×10^5 cfu ml^{-1}. Inoculated plants were kept under high (approximately 95%) humidity, and images were taken 24 h after infiltration. **b**, Col-0 plants were syringe-infiltrated with *Pst*-DC3000, the *avrE1*$^{-}$ mutant, the *hopM1*$^{-}$ mutant or the *avrE1*$^{-}$*/hopM1*$^{-}$ mutant at 2×10^5 cfu ml^{-1}. Inoculated plants were kept under high (approximately 95%) or low (20–40%) humidity. Images were taken 3 days after inoculation. Images are representative of leaves from more than four plants. **c**, **d**, The 6×His:HopM1 transgenic plants[22] were infiltrated with 0.1 nM dexamesathone (DEX), the *avrE1*$^{-}$*/hopM1*$^{-}$ mutant (at 1×10^5 cfu ml^{-1}) or both. H_2O was infiltrated as control. Infiltrated plants were kept at high humidity (approximately 95%). Leaf images were taken 24 h after infiltration (**c**) and bacterial populations were determined 3 days after infiltration (**d**). Significant difference was determined by Student's *t*-test; (two-tailed); ***$P = 1.03 \times 10^{-5}$. $n = 6$ technical replicates from three independent experiments ($n = 2$ in each experiment); data are shown as mean ± s.d.

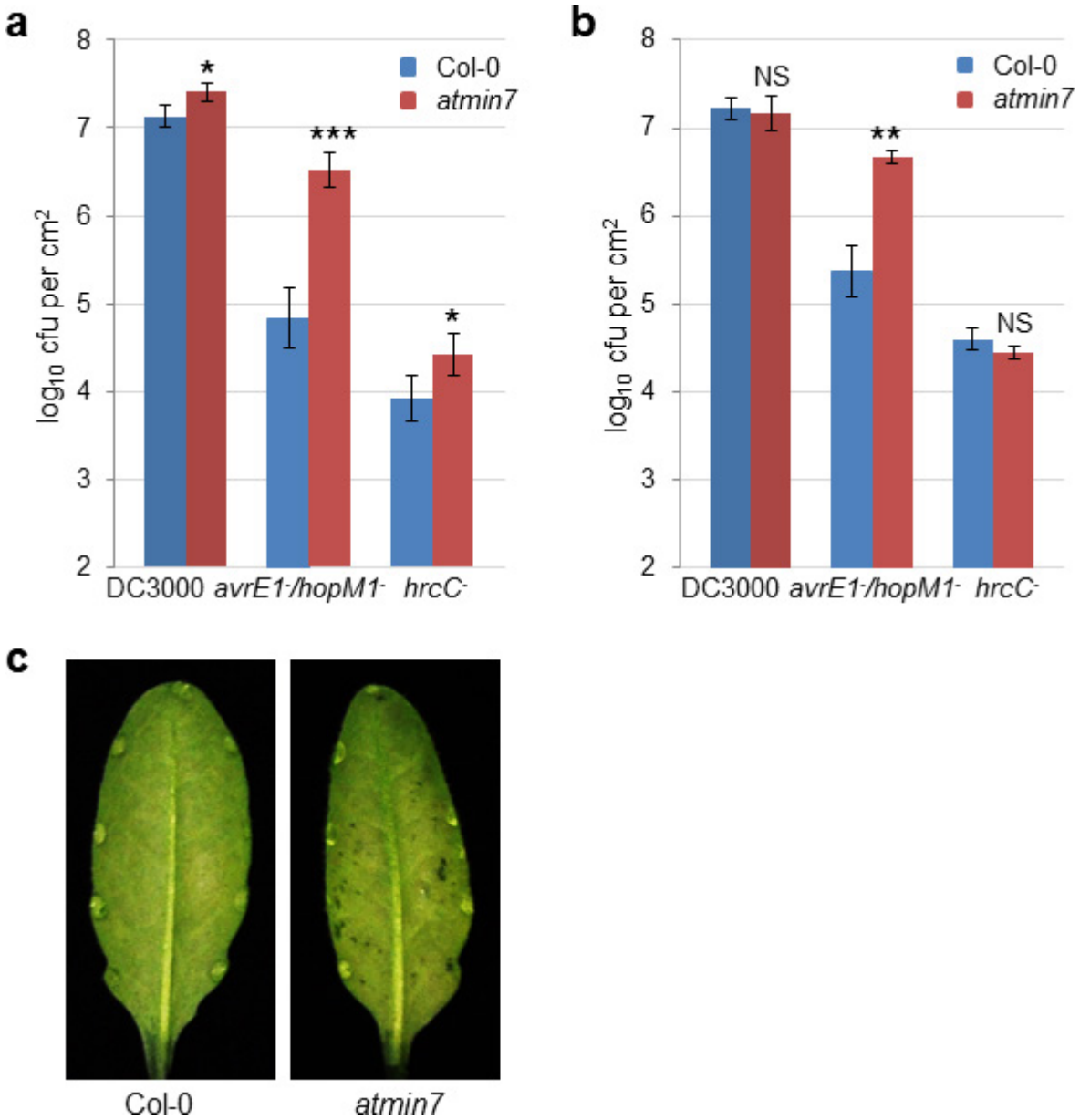

Extended Data Figure 3 | Bacterial multiplication and water soaking in Col-0 and the *atmin7* mutant. a, The Col-0 and *atmin7* plants were dip-inoculated with *Pst*-DC3000, the *avrE1*/*hopM1*$^-$ mutant or the *hrcC*$^-$ mutant at 1×10^8 cfu ml^{-1}. Bacterial populations were determined 4 days after inoculation. Significant difference between Col-0 and *atmin7* plants was determined by Student's *t*-test (two-tailed); $*P = 1.61 \times 10^{-2}$ and 3.12×10^{-2} for DC3000 and *hrcC*$^-$, respectively; $***P = 1.41 \times 10^{-4}$ for *avrE1*$^-$/*hopM1*$^-$. $n = 4$ technical replicates; data are shown as mean ± s.d. Experiments were repeated three times. **b**, **c**, The Col-0 and *atmin7* plants were syringe-infiltrated with *Pst*-DC3000, the *avrE1*$^-$/*hopM1*$^-$ mutant or the *hrcC*$^-$ mutant at 1×10^6 cfu ml^{-1}. Bacterial populations were determined 3 days after inoculation (**b**) and leaf images were taken 38 h after infiltration with the *averE*$^-$/*hopM1*$^-$ mutant strain to show water soaking in *atmin7* leaves (**c**). Significant difference between Col-0 and *atmin7* plants was determined by Student's *t*-test (two-tailed); $**P = 1.63 \times 10^{-3}$ for *avrE1*$^-$/*hopM1*$^-$; NS, not significant ($P = 0.72$ and 0.14 for DC3000 and *hrcC*$^-$, respectively). $n = 3$ technical replicates; data are shown as mean ± s.d. Experiments were repeated three times. Images are representative of leaves from more than four plants.

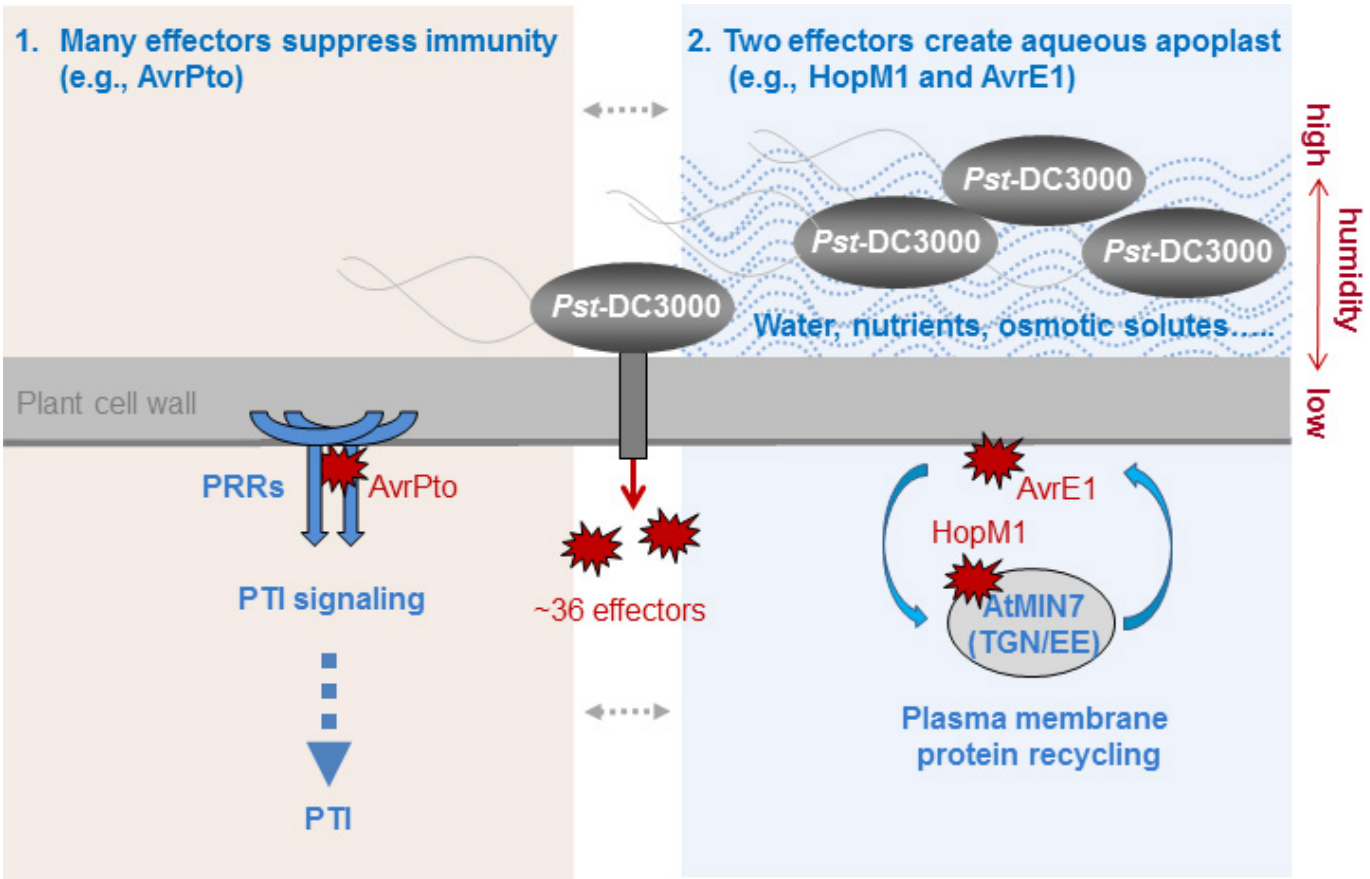

Extended Data Figure 4 | A working model showing the function of HopM1 and AvrE1 in creating aqueous apoplasts. *Pst*-DC3000 delivers a total of 36 effectors into the plant cell. Many effectors, including AvrPto, appear to suppress pattern-triggered immunity (PTI). AvrPto inhibits pattern recognition receptor (PRR) function[8]. Two conserved effectors, HopM1 and AvrE1, create an aqueous apoplast in the presence of bacterial infection in a humidity-dependent manner. AvrE1 is localized to the host plasma membrane[23]. HopM1 targets AtMIN7 (an ARF–GEF protein) in the TGN/EE, which is involved in recycling of plasma membrane proteins[26].

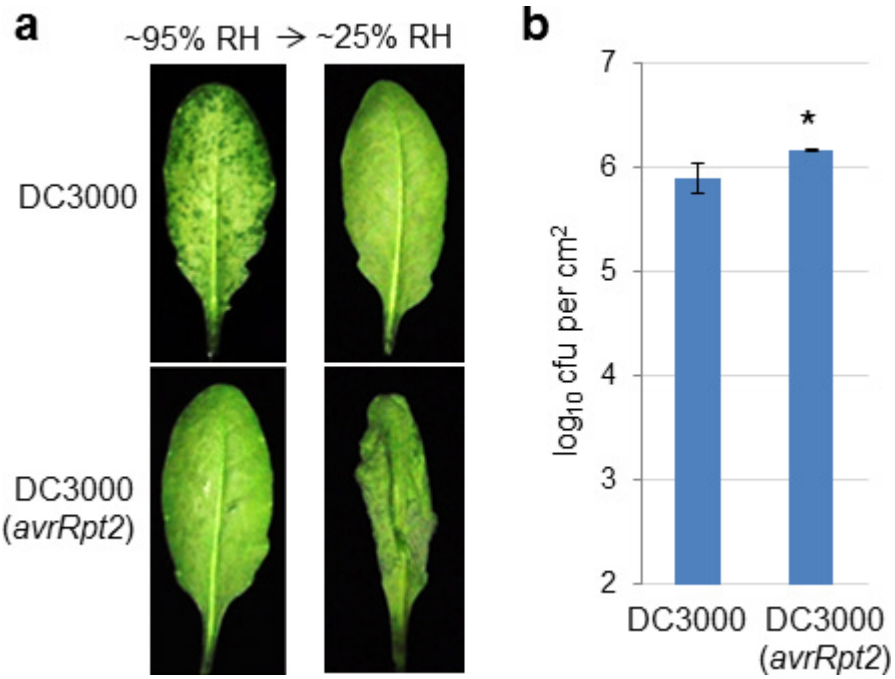

Extended Data Figure 5 | Water-soaking is blocked during ETI. **a**, Col-0 leaves were syringe-infiltrated with *Pst*-DC3000 (1×10^6 cfu ml^{-1}) or *Pst*-DC3000(*avrRpt2*) (1×10^7 cfu ml^{-1}). Plants were kept under high humidity (approximately 95%) for 24 h to observe water soaking and then shifted to low humidity (approximately 25%) for 2 h to observe ETI-associated tissue collapse. Images were taken before and after low humidity exposure (**a**) and bacterial populations were determined 24 h after infiltration to show similar population levels (**b**). Significant difference in bacterial population was determined by Student's *t*-test (two-tailed); $*P = 0.033$. $n = 3$ technical replicates; data are shown as mean ± s.d. Experiments were repeated three times. This is an experimental replicate of Fig. 3b, c (without *rps2* mutant plants).

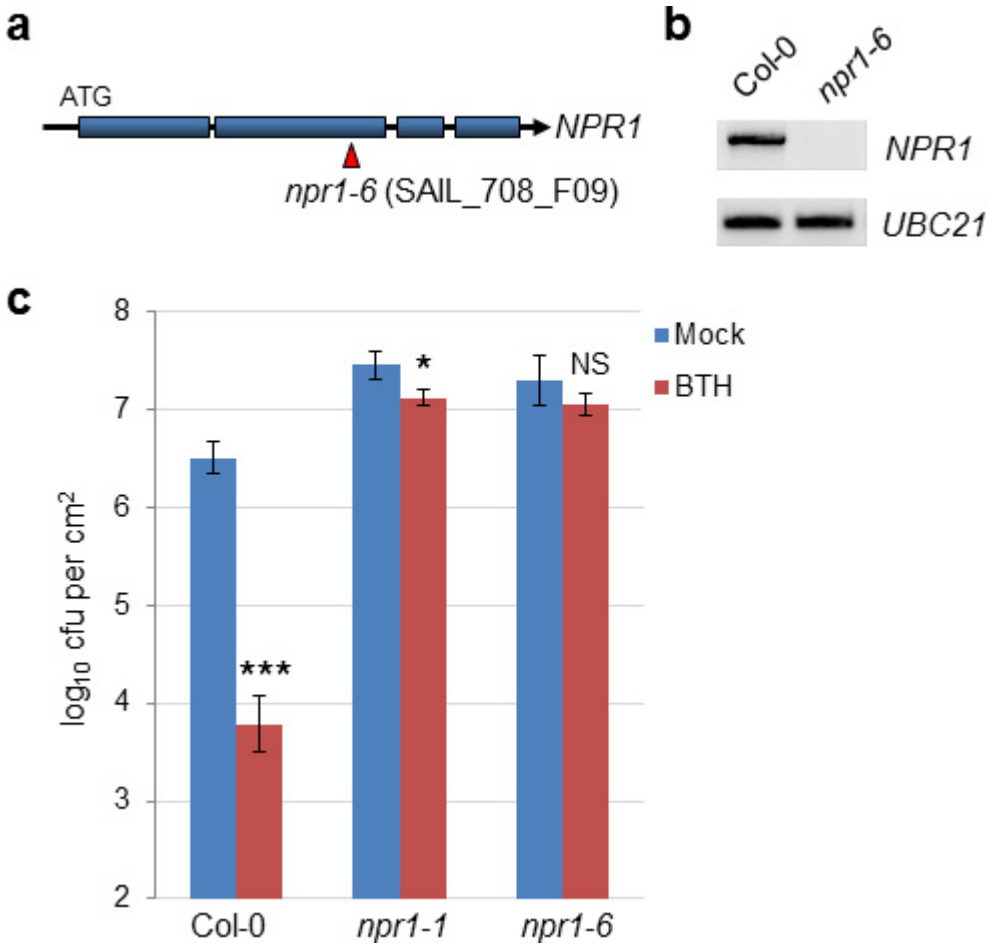

Extended Data Figure 6 | Characterization of the *npr1-6* mutant. **a**, A diagram showing the T-DNA insertion site in the *npr1-6* mutant. Blue boxes indicate exons in the *NPR1* gene. **b**, RT–PCR results showing that the *npr1-6* line cannot produce the full-length *NPR1* transcript. Primers used (*NPR1* sequence is underlined): *NPR1*-F: agaattcATGGACACCACCATTGATGGA; *NPR1*-R: agtcgacCCGACGACGATGAGAGARTTTAC; *UBC21*-F: TCAAATG GACCGCTCTTATC; *UBC21*-R: TCAAATGGACCGCTCTTATC. Uncropped gel images are shown in Supplementary Fig. 1. **c**, The *npr1-6* line, similar to *npr1-1*, is greatly compromised in benzothiadiazole (BTH)-mediated resistance to *Pst*-DC3000 infection. The Col-0, *npr1-1* and *npr1-6* plants were sprayed with 100μM BTH and dip-inoculated with *Pst*-DC3000 at 1×10^8 cfu ml^{-1} 24 h later. Bacterial populations were determined 3 days after inoculation. Significant difference between mock and BTH treatment was determined by Student's *t*-test (two-tailed); $*P = 0.027$; $***P = 1.6 \times 10^{-4}$; NS, not significant ($P = 0.19$). $n = 3$ technical replicates; data are shown as mean ± s.d. Experiments were repeated three times.

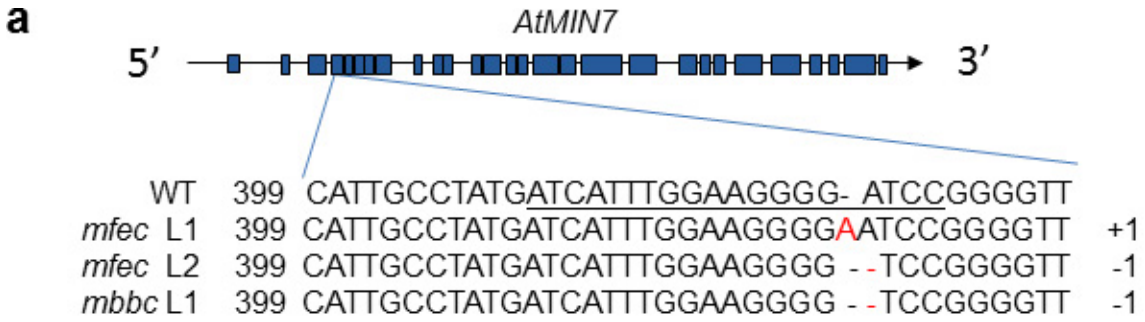

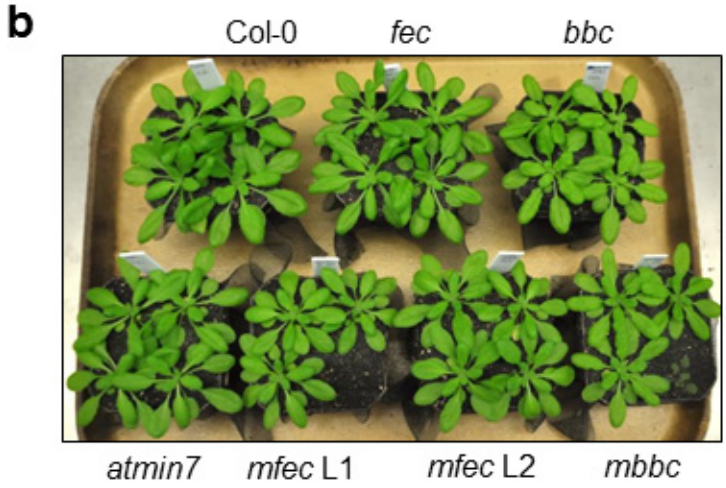

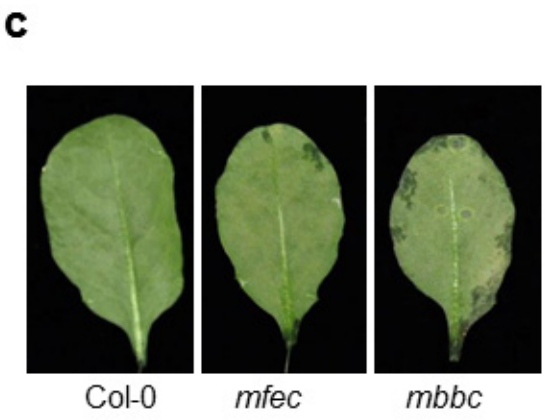

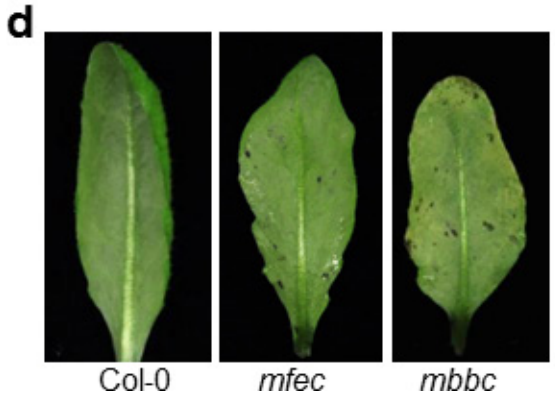

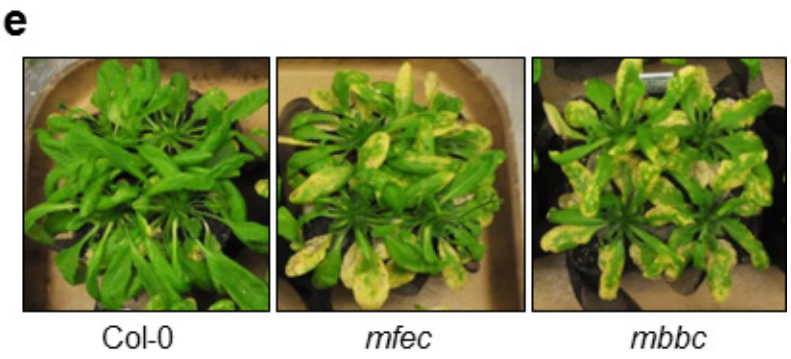

Extended Data Figure 7 | Construction and characterization of the *mfec* and *mbbc* quadruple mutants. a, CRISPR–Cas9-mediated mutations in the 4th exon of the *AtMIN7* gene (exons indicated by blue boxes) in the quadruple mutant lines used in this study. The underlined sequence in the wild type (WT) indicates the region targeted by sgRNA. The number 399 indicates the nucleotide position in the *AtMIN7* coding sequence. +1 and −1 indicate frame shifts in the mutant lines. **b**, Col-0 and various mutants used in this study have similar growth, development and morphology. Four-week-old plants are shown. **c**, The *mfec* and *mbbc* plants show a tendency to develop sporadic water soaking under high humidity. Five-week-old regularly-grown (around 60% relative humidity) Col-0, *mfec* and *mbbc* plants were shifted to high humidity (approximately 95%) overnight and images of mature leaves were taken after the high humidity incubation. **d**, Even leaves of *mfec* and *mbbc* plants that do not have sporadic water soaking have a tendency to develop some water soaking after *hrcC*$^{-}$ inoculation. Five-week-old Col-0, *mfec* and *mbbc* plants were dip-inoculated with *hrcC*$^{-}$ at 1×10^{8} cfu ml^{-1}, and kept under high humidity (approximately 95%). Leaf images were taken 2 days after inoculation. Images are representative of leaves from at least four plants. **e**, The non-pathogenic *hrcC*$^{-}$ mutant causes significant necrosis and chlorosis in the quadruple mutant plants. Col-0, *mfec* and *mbbc* plants were dip-inoculated with the *hrcC*$^{-}$ strain at 1×10^{8} cfu ml^{-1}. Images were taken 9 days after inoculation. This is one of the four independent experimental replications of the results presented in Fig. 5b.

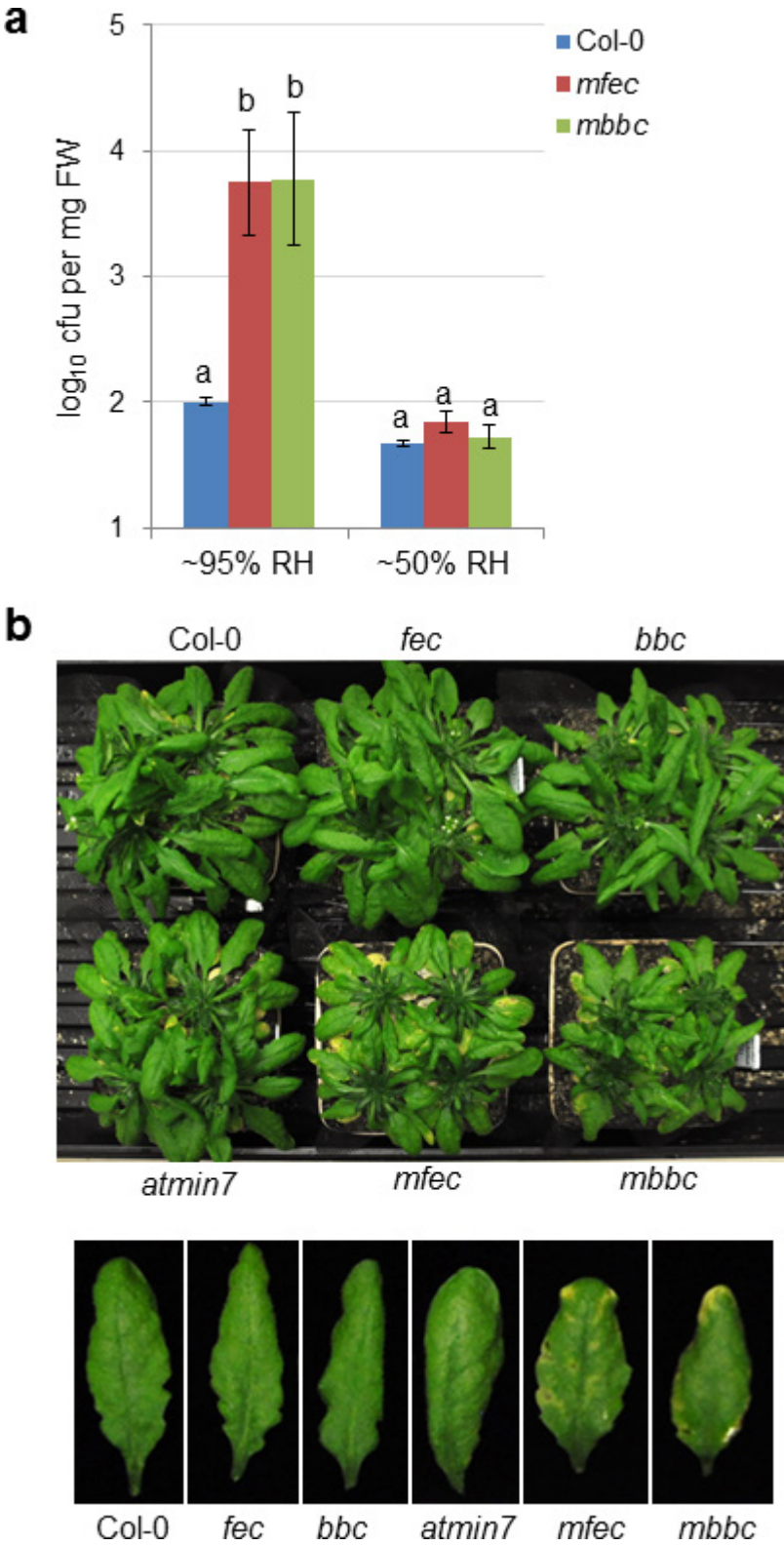

Extended Data Figure 8 | Multiplication of endophytic phyllosphere bacterial community. a, An increase in the endophytic bacterial community in *mfec* and *mbbc* plants depends on high humidity. Col-0, *mfec* and *mbbc* plants were either sprayed with H_2O and kept under high humidity (approximately 95%) or low humidity (around 50%). On day 5, total populations of the endophytic bacterial community were quantified. Statistical analysis was performed by one-way ANOVA with Tukey's test (significance set at $P \leq 0.05$). Bacterial populations indicated by different letters (a and b) are significantly different. $n = 4$ technical replicates; data are shown as mean ± s.d. Experiments were repeated three times. **b**, Mild chlorosis and necrosis in leaves is associated with increased endophytic bacterial community level in the *mfec* and *mbbc* quadruple mutant plants. Plants were sprayed with H_2O and kept under high (approximately 95%) humidity. Images were taken 10 days after spraying. Individual leaves are enlarged and shown in the lower panel, showing mild chlorosis and necrosis in some of the *mfec* and *mbbc* leaves.

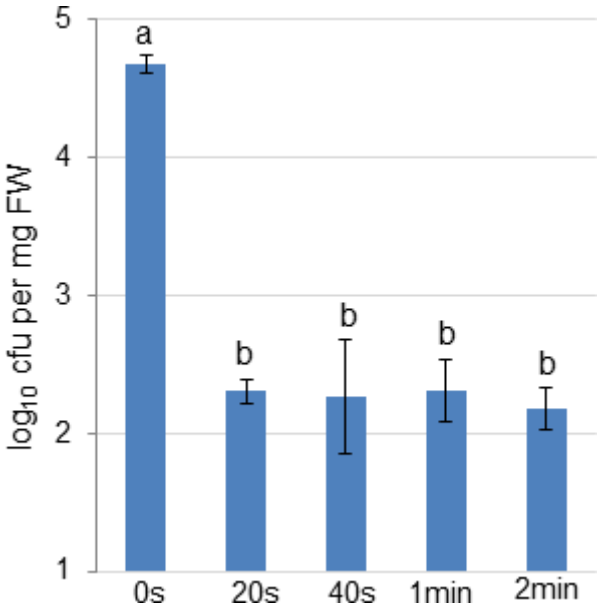

Extended Data Figure 9 | Validation of 1 min as an effective surface sterilization time. Five-week-old Col-0 plants were sprayed with H_2O and kept under high humidity (approximately 95%) for 5 days. Leaves were detached, surface sterilized in 75% ethanol for 20 s, 40 s, 1 min or 2 min and then rinsed in sterile water twice. No sterilization (0 s) was used as control. Leaves were ground in sterile water and bacterial numbers were determined by serial dilutions and counting of colony-forming units on R2A plates. Statistical analysis was performed by one-way ANOVA with a Tukey's test (significance set at $P \leq 0.05$). Bacterial populations indicated by different letters (that is, a and b) are significantly different. $n = 4$ technical replicates; data are shown as mean ± s.d. Experiments were repeated twice with similar results.

Extended Data Table 1 | Endophytic bacterial taxa in Col-0, *mfec* and *mbbc* plants

Order/Family	Col-0	*mfec*	*mbbc*
Bacillales			
Paenibacillaceae	15 (30%)	ND	ND
Burkholderiales			
Comamonadaceae	8 (16%)	12 (24%)	9 (18%)
Burkholderiaceae	4 (8%)	1 (2%)	22 (44%)
Alcaligenaceae	3 (6%)	19 (38%)	12 (24%)
Flavobacteriales			
Flavobacteriaceae	6 (12%)	1 (2%)	1 (2%)
Xanthomonadales			
Xanthomonadaceae	4 (8%)	9 (18%)	ND
Sphingomonadales			
Sphingomonadaceae	3 (6%)	ND	1 (2%)
Sphingobacteriales			
Sphingobacteriaceae	3 (6%)	ND	ND
Chitinophagaceae	1 (2%)	ND	ND
Rhizobiales			
Rhizobiaceae	2 (4%)	5 (10%)	ND
Cytophagales			
Cytophagaceae	1 (2%)	ND	ND
Pseudomonadales			
Pseudomonadaceae	ND	1 (2%)	5 (10%)
Actinomycetales			
Microbacteriaceae	ND	2 (4%)	ND

ND, not detected. See Methods for 16S rRNA amplicon sequencing procedures.